Estimating Red Leak in FUV Band of UVIT from in Orbit Spectral Observations

S N Tandon, and Gulab Dewangan, IUCAA, Pune

December 11, 2022

1. Introduction

Ultraviolet imaging telescope (UVIT) is primarily designed for imaging in FUV (1250-1800 A) and NUV (2000-3000 A). The field of view is ~ 28′ diameter and the spatial resolution obtained is ~ 1.5″. The wavelength range for each detector is defined by appropriate solar blind photo-cathode for rejection of the longer wavelengths and suitable windows to absorb shorter wavelengths. A set of filters is provided for each of the two broad bands for selection of a narrower wavelength range. In the FUV band selection of narrower range is done through long pass filters which absorb shorter wavelengths, while the longer wavelengths are rejected by the photo-cathode. In addition to the filters, gratings are provided for slit less spectroscopy with a low resolution of ~ 80. For more details see Tandon et al (2017) and Tandon et al (2020).

As a convention, the upper and lower limits of the wavelength mentioned for any filter in a telescope refer to the wavelengths where the transmission is significant, and outside these limits the transmission, if at all, is very small. The pass bands for imaging in FUV are documented as having an upper limit on the wavelength as 1800 A. While for most of the observation, the conclusions are not affected materially by the small transmission for > 1800 A, in some studies small transmission of the longer wavelengths, which have much larger fluxes, can be important. As an example, if one is looking for small flux of Lyman continuum radiation from galaxies, small red leak in FUV for wavelengths > 1800 A, if ignored, could lead to erroneous conclusions. In this paper we present estimates of red leak in FUV, of wavelengths > 1800 A, from in-orbit spectral observations of planetary nebula NGC40. In the next section we describe the data used and explain estimation of the effective area for the leak. In the third section we discuss the results obtained, and in the last section the conclusions are presented.

2. Data used and the procedure for estimating effective area for the leak

Spectral observations of the nucleus of planetary nebula NGC40 are used for estimating red-leak at wavelengths > 1800 A. Window of the detector (MgF_2) does not transmit any radiation for wavelengths < 1200 A. Thus, the spectral trail of the first order has no mix up with the second order for wavelengths < 2400 A. However, some scattered light could reach locations of the wavelengths 1800 – 2400 A in the first order. The scattered light is expected to give a smoothly varying signal. Therefore, if the source has sharp emission lines over a continuum then enhancement at the corresponding location in the observed spectral trail, over the underlying continuum, can be taken as extra signal due to the line alone, even in the presence of scattered light. The low resolution IUE spectrum of this source shows sharp emission lines at ~ 1908.6 A with two weak lines in its neighbourhood at ~ 1894 A and 1924 A, and at 2898.5 A (see Feibelman,1999). Thus, measurement of the enhancement in the spectral trail at the corresponding location is a good estimate of the leaked signal from these lines.

The observed spectral trails for NGC40 (Observation ID: C07_015T01_9000005256) are shown in Fig. 1. The wavelength scale shown is based on the calibration given in Dewangan (2021). The calibration given there is valid for the wavelength range 1300 A to 1800 A, but for wavelengths > 1800 A a different approach was needed by fitting the grating equation as per geometrical relation between the grating and the detector. This change in effect shifts the wavelength 2300 A by ~ 10 A which can be compared with the resolution of ~ 40 A for the first order. The data on the spectral trails and correction on the wavelength are also shown in the Appendix 1 for relevant wavelengths.

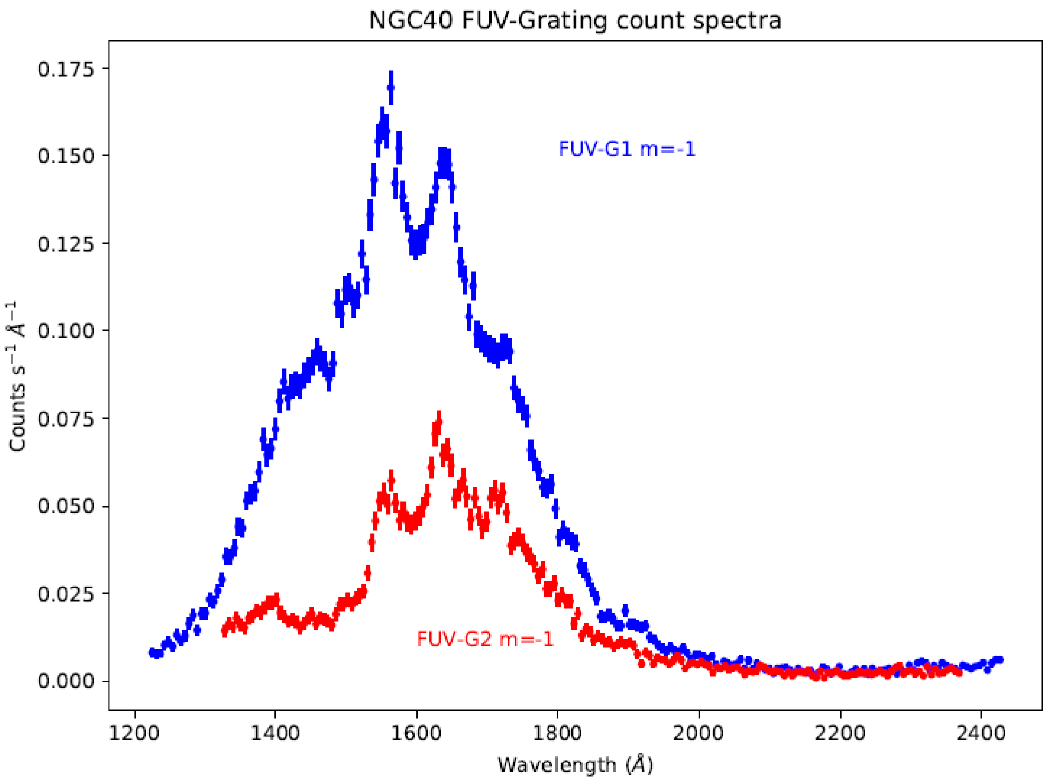

Fig. 1 Observed spectral trails of NGC40, for the first order, are shown for the two FUV gratings. Emission lines for wavelengths < 1800 A are seen as prominent enhancements, while the emission line at 1908.6 A is seen as a small enhancement and the line at 2898.5 A is not visible.

The following procedure is used to estimate enhancement due to the line: a) it is assumed that signal due to the line is restricted within a window with an extension of ~ 35 A on either side of the main line at 1908.6 A which has two minor lines close by at 1894.2 A and 1924.2 A respectively, and to within ~ 25 A on either side of the line at 2298.8 A, b) the continuum underlying the line is found by fitting a third order polynomial to the signals within ~ 50 A on each side of the window mentioned for the line in “a)”, c) use the fit obtained in “b)” to calculate the total signal of the continuum within the window mentioned in “a)”, and d) from the total signal within the window subtract the total signal found in “c)”. The results obtained are shown in Table 1. Total signal in the IUE spectrum for the lines is taken from Feibelman (1999). A comparison of the enhancement for the lines in the spectrum obtained with UVIT and the total signal in the lines as per Feibelman (1999) gives effective area of the grating at the corresponding wavelength. All the filters except Sapphire have a transmission of 90% at these wavelengths (see Astrosat Handbook V1.11, 2018) which is much higher than efficiency of the grating. Therefore, to get the effective area in imaging mode a correction is made assuming a transmission of 90% for the filters and taking efficiency of the grating from the ground calibration (*see* *https://uvit.iiap.res.in/Instrument/Gratings*). The results are shown in Table 1. The weighted average of the two estimated effective areas for imaging in FUV are: 0.345 +- 0.033 sq cm and 0.060+-0.02 sq cm for 1908.6 A and 2298.8 A respectively.

FUV-Grating1	[a] 1908.6A	1.094, 0.025	0.841	0.25, 0.025	12.17	1.17	0.21, 0.021	0.40, 0.04
FUV-Grating2	[a] 1908.6A	0.6534, 0.025	0.5605	0.093, 0.025	12.17	1.17	0.079, 0.02	0.22, 0.06
FUV-Grating1	2298.8A	0.194, 0.016	0.171	0.023, 0.016	7.08	0.82	0.028, 0.02	0.059, 0.04
FUV-Grating2	2298.8A	0.129, 0.01	0.105	0.024, 0.01	7.08	0.82	0.029, 0.012	0.061, 0.025

[a]) The data for this line includes contribution from the two minor lines at 1894.2 A and 1924.2 A.

Table 1: Results on estimation of effective areas at 1908.6 A and 2298.8 A are shown. First column shows the grating, second column shows the wavelength in A, third column shows the total C/S observed within a window centred on the line, fourth column shows estimated C/S for continuum in the window centred on the line, fifth column shows estimated C/S in the line, sixth column shows flux in the line in units “10^-12 ergs/(s. sq cm)” as given by Feibelman (1999), seventh column gives value of the sixth column in units of “photon counts/(s. sq cm)”, eighth column gives effective area in” sq cm” for the grating, and the last column gives the estimated effective area in “sq cm” for the imaging mode. The second number in any cell is the error on the first number.

3. Discussion

The results obtained here can be compared with what can be expected from other measurements. From the curve of sensitivity for CsI photo-cathode, given as curve 100M in Fig 4.2-b of "Photomultiplier Tubes, Basics and Application, Hamamatsu, 3rd edition, 2006, we infer that variation in the QE between 1600 A and 2000 A is a power law with slope "- 14.43". If we use results of ground calibration for the effective area at 1600 A and apply normalisation correction to it found in the in-orbit calibration (Tandon et al, 2020), and combine it with the effective area obtained here for 1908.6 A, after due consideration of the lower transmission of the filter at 1600 A, a slope of "-19.65" is obtained for the power law. The present estimates of effective area at 1908.3 A and 2300 A can be fitted by a power law with slope "-9.4". As the transmission of the detector's window is almost constant at ~ 90% for all these wavelengths, the QE and effective area have identical wavelength dependence. Thus it appears that the direct measurements of the effective area show a slower decline with increasing wavelength as compared to the indirect indications. Therefore we can take the estimate made here, i.e. "Effective area = 0.345 * (λ A/1908.3)^-9.4 sq cm" as upper bound for the red leak at wavelengths > 1908.6 A. Further, a power law can be used to estimate effective area between 1800 A and 1908.6 A, i.e. "Effective area = 0.345 * (λ A/1908.6)^ (-19.65) sq cm"

4. Conclusion

An estimate of the effective area of imaging mode in FUV in UVIT has been made, from observations of NGC40 in spectral mode, at 1908.6 A and 2298.8 A. Based on these estimates and the ground calibration for the effective areas normalised with in-orbit calibration, it is concluded that the effective area for imaging mode of FUV in UVIT can be taken as: i)" 0.345 * (λ A/1908.3)^-9.4 sq cm" for wavelengths between 1908.6 and 2298.8", and ii) "0.345 *(λ A/1908.6)^-19.65" for wavelengths between 1800 A and 1908.6 A. Further, for wavelengths > 2300 A, in the absence any other estimate available, formula "i)" can be used.

Acknowledgements:

…

References

Astrosat Handbook V1.11, Space Science Programme Office (SSPO)
INDIAN SPACE RESEARCH ORGANISATION (ISRO), HQ, (2021)

Dewangan G. C., J. Astrophys. Astr. 42, 49 (2021)

Feibelman W. A.
The Astrophysical Journal, 514, 296 (1999)

Tandon S.N., Subramaniam A., Girish V., Postma, J., et al
The Astronomical Journal, 154, 128, (2017).

Tandon S. N., Postma J., Joseph P., Devaraj A. et al
The Astronomical Journal, 159, 158 (2020)

Appendix 1: Observed Counts per second for spectral observation of NGC40 in the 1st order. The Columns "Corrected wavelength" show the wavelengths obtained after recalibration using the grating equation. (source of the observed counts Devangan G. , Nov 22)

Counts in the spectrum of NGC 40 with Grating 1 FUV				Counts in the spectrum of NGC40 with Grating 2 FUV			
Wave-length in A	Counts per second per A C/(S.A)	Error on C/(S.A)	Cor-rected wave-length in A	Wave-length in A	Counts per second per A C/(S.A)	Error on C/(S.A)	Cor-rected wave-length in A
2426.08	0.0060219	0.000988	2414.621	2368.32	0.00222948	0.000645	2380.51
2420.24	0.0060152	0.000932	2408.913	2362.69	0.00281967	0.000823	2374.8
2414.41	0.005081	0.000942	2403.205	2357.07	0.00370889	0.000823	2369.09
2408.58	0.0030806	0.000765	2397.496	2351.44	0.00312468	0.000824	2363.38
2402.74	0.0052214	0.000893	2391.787	2345.82	0.00236709	0.000693	2357.67
2396.91	0.0044064	0.000852	2386.077	2340.19	0.00208283	0.000694	2351.96
2391.08	0.0041561	0.000789	2380.367	2334.57	0.00340555	0.000823	2346.25
2385.24	0.0034711	0.000776	2374.657	2328.94	0.00178242	0.000694	2340.53

2379.41	0.0041397	0.000831	2368.946	2323.31	0.00401206	0.000875	2334.82
2373.58	0.0045413	0.000863	2363.235	2317.69	0.00148528	0.000626	2329.11
2367.75	0.002945	0.000679	2357.523	2312.06	0.00281893	0.000709	2323.39
2361.91	0.003602	0.000765	2351.811	2306.44	0.00209757	0.000837	2317.68
2356.08	0.0038827	0.000788	2346.099	2300.81	0.00296633	0.000781	2311.96
2350.25	0.0044217	0.000854	2340.386	2295.19	0.0028269	0.000823	2306.25
2344.41	0.0052181	0.000853	2334.673	2289.56	0.00194209	0.000645	2300.53
2338.58	0.0036188	0.000765	2328.96	2283.94	0.00430733	0.001013	2294.82
2332.75	0.0044159	0.000832	2323.246	2278.31	0.00385409	0.000862	2289.1
2326.91	0.0032024	0.000799	2317.532	2272.69	0.00282906	0.00074	2283.38
2321.08	0.0050764	0.000941	2311.817	2267.06	0.00148889	0.000724	2277.67
2315.25	0.005628	0.000943	2306.102	2261.43	0.00223687	0.000824	2271.95
2309.41	0.0052114	0.000933	2300.387	2255.81	0.00296416	0.000724	2266.23
2303.58	0.0032068	0.000777	2294.671	2250.18	0.0022298	0.000739	2260.51
2297.75	0.0045477	0.000821	2288.955	2244.56	0.00177941	0.000753	2254.79
2291.91	0.0026719	0.000754	2283.239	2238.93	0.00251968	0.000709	2249.07
2286.08	0.0030699	0.000764	2277.522	2233.31	0.00208341	0.000554	2243.36
2280.25	0.0020063	0.000665	2271.805	2227.68	0.00267515	0.000724	2237.64
2274.41	0.0032189	0.000777	2266.088	2222.06	0.00193684	0.000796	2231.92
2268.58	0.0036104	0.00081	2260.37	2216.43	0.00192971	0.000644	2226.2
2262.75	0.003212	0.000777	2254.651	2210.81	0.00149597	0.000662	2220.47
2256.91	0.0030667	0.000853	2248.933	2205.18	0.00148856	0.00066	2214.75
2251.08	0.0025503	0.000788	2243.214	2199.55	0.00207495	0.000753	2209.03
2245.25	0.0036125	0.000788	2237.495	2193.93	0.00297042	0.000725	2203.31
2239.41	0.0018736	0.000706	2231.775	2188.3	0.00223314	0.000823	2197.59
2233.58	0.0034776	0.000729	2226.055	2182.68	0.0023772	0.000724	2191.87
2227.75	0.0022772	0.000692	2220.334	2177.05	0.00089979	0.000724	2186.14
2221.92	0.0034825	0.00068	2214.614	2171.43	0.00267885	0.000694	2180.42
2216.08	0.0026736	0.000625	2208.892	2165.8	0.00089348	0.000661	2174.7

2041.09	0.004953	0.000894	2037.095	1997.04	0.00475095	0.000958	2002.83
2035.25	0.0056279	0.000923	2031.364	1991.41	0.00519214	0.000924	1997.1
2029.42	0.0036115	0.000766	2025.631	1985.79	0.00475191	0.000959	1991.36
2023.59	0.0048127	0.000903	2019.899	1980.16	0.00356713	0.00081	1985.63
2017.75	0.0070802	0.001005	2014.166	1974.54	0.00593423	0.001126	1979.89
2011.92	0.0062894	0.000951	2008.433	1968.91	0.00712918	0.001067	1974.16
2006.09	0.0070959	0.00109	2002.7	1963.28	0.00577924	0.000991	1968.42
2000.25	0.0075001	0.001032	1996.966	1957.66	0.00488283	0.000946	1962.68
1994.42	0.0073624	0.001041	1991.232	1952.03	0.00593211	0.000958	1956.95
1988.59	0.0062797	0.001005	1985.497	1946.41	0.0060828	0.000992	1951.21
1982.75	0.0080356	0.001066	1979.762	1940.78	0.00667069	0.001116	1945.47
1976.92	0.0095081	0.001199	1974.027	1935.16	0.0048996	0.00097	1939.74
1971.09	0.0082775	0.001098	1968.292	1929.53	0.00725493	0.001116	1934
1965.25	0.0085567	0.001114	1962.556	1923.91	0.00813505	0.001209	1928.26
1959.42	0.0096328	0.001176	1956.82	1918.28	0.00489241	0.000969	1922.52

1953.59	0.0084244	0.001138	1951.084	1912.66	0.0076938	0.0012	1916.78
1947.75	0.0093626	0.001161	1945.347	1907.03	0.01006226	0.001288	1911.05
1941.92	0.0100356	0.001228	1939.61	1901.4	0.01095912	0.001338	1905.31
1936.09	0.0118892	0.001325	1933.873	1895.78	0.01050434	0.001345	1899.57
1930.26	0.0125833	0.001385	1928.135	1890.15	0.01111649	0.001441	1893.83
1924.42	0.0156697	0.001442	1922.397	1884.53	0.01064011	0.001369	1888.09
1918.59	0.0153891	0.001501	1916.659	1878.9	0.00993112	0.001228	1882.35
1912.76	0.0158074	0.001508	1910.92	1873.28	0.01125184	0.001321	1876.61
1906.92	0.0160313	0.001494	1905.181	1867.65	0.01095252	0.00137	1870.87
1901.09	0.0160441	0.001471	1899.442	1862.03	0.01197913	0.001362	1865.12
1895.26	0.0200567	0.001653	1893.703	1856.4	0.01271721	0.001506	1859.38
1889.42	0.0157725	0.001542	1887.963	1850.78	0.01167911	0.001377	1853.64
1883.59	0.0157722	0.001483	1882.223	1845.15	0.01405791	0.001514	1847.9
1877.76	0.0177986	0.001582	1876.482	1839.52	0.01492716	0.001624	1842.16
1871.92	0.0189839	0.001631	1870.742	1833.9	0.01302471	0.001448	1836.41
1866.09	0.0181791	0.001598	1865	1828.27	0.0192282	0.001735	1830.67
1860.26	0.0184643	0.00161	1859.259	1822.65	0.01638524	0.00161	1824.93
1854.42	0.0235237	0.001796	1853.517	1817.02	0.02275643	0.001902	1819.18
1848.59	0.0260626	0.001879	1847.776	1811.4	0.02261405	0.001838	1813.44
1842.76	0.0290054	0.001989	1842.033	1805.77	0.0245638	0.001949	1807.69
1836.92	0.0316925	0.00211	1836.291	1800.15	0.02307736	0.001891	1801.95
1831.09	0.0328421	0.002138	1830.548	1794.52	0.0278063	0.002089	1796.2
1825.26	0.0391483	0.00231	1824.805	1788.89	0.02617726	0.002041	1790.46
1819.42	0.0398664	0.002315	1819.061	1783.27	0.02629406	0.002087	1784.71
1813.59	0.041324	0.002357	1813.318	1777.64	0.0319207	0.002249	1778.97
1807.76	0.0433117	0.002448	1807.573	1772.02	0.02985419	0.002119	1773.22
1801.92	0.0410326	0.002386	1801.829	1766.39	0.03340647	0.002268	1767.48